

# Solution Calorimetric and Stopped-Flow Kinetic Studies of the Reaction of $\bullet\text{Cr}(\text{CO})_3\text{C}_5\text{Me}_5$ with $\text{PhSe-SePh}$ and $\text{PhTe-TePh}$ . Experimental and Theoretical Estimates of the Se–Se, Te–Te, H–Se, and H–Te Bond Strengths

James E. McDonough, John J. Weir, Matthew J. Carlson, and Carl D. Hoff\*

Department of Chemistry, University of Miami, 1301 Memorial Drive, Coral Gables, Florida 33146

Olga P. Kryatova and Elena V. Rybak-Akimova\*

Department of Chemistry, Tufts University, 62 Talbot Avenue, Medford, Massachusetts 02155

Christopher R. Clough and Christopher C. Cummins\*

Department of Chemistry, Massachusetts Institute of Technology, Rm. 2-227, 77 Massachusetts Avenue, Cambridge, Massachusetts 02139

Received November 28, 2004

The kinetics of the oxidative addition of  $\text{PhSeSePh}$  and  $\text{PhTeTePh}$  to the stable 17-electron complex  $\bullet\text{Cr}(\text{CO})_3\text{C}_5\text{Me}_5$  have been studied utilizing stopped-flow techniques. The rates of reaction are first-order in each reactant, and the enthalpy of activation decreases in going from Se ( $\Delta H^\ddagger = 7.0 \pm 0.5$  kcal/mol,  $\Delta S^\ddagger = -22 \pm 3$  eu) to Te ( $\Delta H^\ddagger = 4.0 \pm 0.5$  kcal/mol,  $\Delta S^\ddagger = -26 \pm 3$  eu). The kinetics of the oxidative addition of  $\text{PhSeH}$  and  $\bullet\text{Cr}(\text{CO})_3\text{C}_5\text{Me}_5$  show a change in mechanism in going from low (overall third-order) to high (overall second-order) temperatures. The enthalpies of the oxidative addition of  $\text{PhE-EPh}$  to  $\bullet\text{Cr}(\text{CO})_3\text{C}_5\text{Me}_5$  in toluene solution have been measured and found to be  $-29.6$ ,  $-30.8$ , and  $-28.9$  kcal/mol for S, Se, and Te, respectively. These data are combined with enthalpies of activation from kinetic studies to yield estimates for the solution-phase  $\text{PhE-EPh}$  bond strengths of 46, 41, and 33 kcal/mol for  $\text{E} = \text{S}$ ,  $\text{Se}$ , and  $\text{Te}$ , respectively. The corresponding  $\text{Cr-EPh}$  bond strengths are 38, 36, and 31 kcal/mol. Two methods have been used to determine the enthalpy of hydrogenation of  $\text{PhSeSePh}$  in toluene on the basis of reactions of  $\text{HSPH}$  and  $\text{HSePh}$  with either  $\bullet\text{Cr}(\text{CO})_3\text{C}_5\text{Me}_5$  or 2-pyridine thione. These data lead to a thermochemical estimate of 72 kcal/mol for the  $\text{PhSe-H}$  bond strength in toluene solution, which is in good agreement with kinetic studies of H atom transfer from  $\text{HSePh}$  at higher temperatures. The reaction of  $\text{H-Cr}(\text{CO})_3\text{C}_5\text{Me}_5$  with  $\text{PhSe-SePh}$  is accelerated by the addition of a Cr radical and occurs via a rapid radical chain reaction. In contrast, the reaction of  $\text{PhTe-TePh}$  and  $\text{H-Cr}(\text{CO})_3\text{C}_5\text{Me}_5$  does not occur at any appreciable rate at room temperature, even in the presence of added Cr radicals. This is in keeping with a low  $\text{PhTe-H}$  bond strength blocking the chain and implies that  $\text{H-TePh} \leq 63$  kcal/mol. Structural data are reported for  $\text{PhSe-Cr}(\text{CO})_3\text{C}_5\text{Me}_5$  and  $\text{PhS-Cr}(\text{CO})_3\text{C}_5\text{Me}_5$ . The two isostructural complexes do not show signs of an increase in steric strain in terms of metal–ligand bonds or angles as the  $\text{Cr-EPh}$  bond is shortened in going from Se to S. Bond strength estimates of the  $\text{PhE-H}$  and  $\text{PhE-EPh}$  derived from density functional theory calculations are in reasonable agreement with experimental data for  $\text{E} = \text{Se}$  but not for  $\text{E} = \text{Te}$ . The nature of the singly occupied molecular orbital of the  $\bullet\text{EPh}$  radicals is calculated to show increasing localization on the chalcogenide atom in going from S to Se to Te.

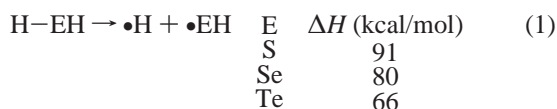
## Introduction

The availability of thermodynamic data on the  $\text{RE-ER}$  and  $\text{RE-H}$  bonds drops off rapidly in going from  $\text{E} = \text{O}$  to S and is virtually absent for Se and Te. Gas-phase first bond

dissociation energies for  $\text{H}_2\text{E}$  are available and represent the most accurate data available for the heavier chalcogenides,

\* Authors to whom correspondence should be addressed. E-mail: c.hoff@miami.edu (C.D.H.).

as shown in eq 1:<sup>11</sup>



It is worth noting that although hydrogenation of elemental sulfur is exothermic ( $\Delta H^\circ_f$  of  $\text{H}_2\text{S} = -4.9$  kcal/mol), it is endothermic for both  $\text{H}_2\text{Se}$  ( $\Delta H^\circ_f = +7.1$  kcal/mol) and  $\text{H}_2\text{Te}$  ( $\Delta H^\circ_f = +23.8$  kcal/mol)<sup>2</sup>.

These periodic trends would be expected to show up in the thermodynamics of the oxidative addition/reductive elimination of hydrogen to organic dichalcogenides.



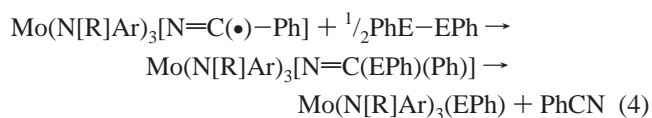
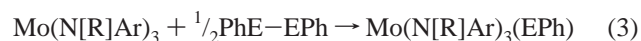
Except for sulfur, experimental data of use in eq 2 is severely limited.<sup>3</sup> The enthalpy of reaction 2 for  $\text{E} = \text{S}$ , with all species in toluene solution, is  $-11$  kcal/mol.<sup>4</sup> This provides a method to derive the  $\text{PhS-SPh}$  bond strength provided the  $\text{H-ER}$  bond strength is known. Bordwell and co-workers have utilized  $\text{p}K_a$  and electrochemical data to estimate the  $\text{H-SPh}$  bond strength as  $79$  kcal/mol.<sup>5</sup> We have previously used these data together with enthalpies of formation and solution to estimate the  $\text{PhS-SPh}$  bond dissociation enthalpy to be  $43$  kcal/mol in toluene solution.<sup>4</sup> Photoacoustic calorimetric (PAC) studies<sup>6</sup> have recently yielded a higher estimate of the  $\text{PhS-H}$  bond strength in solution of  $83.5$  kcal/mol, which would yield an estimate of  $51$  kcal/mol for the  $\text{PhS-SPh}$  bond strength in toluene solution (see ref 6b). This compares to an earlier estimate of  $40.6$  kcal/mol made by Griller and co-workers<sup>7</sup> and to a gas-phase value quoted

- (1) (a) Blanksby, S. J.; Ellison, G. B. *Acc. Chem. Res.* **2003**, *36*, 255. (b) Gibson, S. T.; Greene, J. P.; Berkowitz, J. J. *Chem. Phys.* **1986**, *85*, 4815. (c) Sablier, M.; Fujii, T. *Chem. Rev.* **2002**, *102*, 2855. (d) *CRC Handbook of Chemistry and Physics*, 84th edition; Lide, D. R., Ed.; CRC Press: Boca Raton, FL, 2003–2004.
- (2) (a) Wagman, D. D.; Evans, W. H.; Parker, V. B.; Schumm, R. H.; Halow, I.; Bailey, S. M.; Churney, K. L.; Nuttall, R. R. *J. Chem. Phys. Ref. Data* **1982**, *11* (Suppl. 2). (b) NIST Chemistry WebBook. <http://webbook.nist.gov>
- (3) A value of  $66.9$  kcal/mol has been reported for the  $\text{PhSe-SePh}$  bond strength on the basis of enthalpy of combustion data; however, it seems unlikely that this bond is stronger than the  $\text{PhS-SPh}$  bond. The authors could not find data for  $\text{PhTe-TePh}$ . Mortimer, C. T.; Waterhouse, J. *J. Chem. Thermodyn.* **1980**, *12*, 961.
- (4) Mukerjee, S. L.; Gonzalez, A. A.; Nolan, S. P.; Ju, T. D.; Lang, R. F.; Hoff, C. D. *Inorg. Chim. Acta* **1995**, *240*, 175.
- (5) Bordwell, F. G.; Zhang, X. M.; Satish, A. V.; Cheng, J. P. *J. Am. Chem. Soc.* **1994**, *116*, 6605.
- (6) (a) Santos, R. M. B. D.; Muralha, V. S. F.; Correia, C. F.; Guedes, R. C.; Cabral, B. J. C.; Simoes, J. A. M. *J. Phys. Chem.* **2002**, *106*, 9883. (b) Estimates of the  $\text{PhS-H}$  and  $\text{PhS-SPh}$  bonds interrelate through enthalpy of hydrogenation values as noted in ref 4. The value of  $83.5$  kcal/mol for the  $\text{PhS-H}$  bond in ref 6a leads to an estimate of  $51.8$  kcal/mol for the  $\text{PhS-SPh}$  bond strength in solution using the method described in ref 4. The value of  $\text{PhS-SPh}$  reported later in this work of  $46$  kcal/mol for the  $\text{PhS-SPh}$  bond in toluene solution would lead to an estimate of  $80.5$  kcal/mol for the solution phase  $\text{PhS-H}$  bond strength. This is roughly between the value of Bordwell (ref 5) of  $79$  and the PAC value of  $83.5$  (ref 6a). At this time, an estimate of  $81 \pm 3$  kcal/mol seems reasonable for the solution phase  $\text{PhS-H}$  bond strength estimate. A more precise analysis will require a better understanding of the solvation enthalpy of the  $\text{PhS}$  radical than is currently available. In addition, there are experimental errors in all of the measurements utilized in these estimates.
- (7) Griller, D.; Barclay, L. R. C.; Ingold, K. U. *J. Am. Chem. Soc.* **1975**, *97*, 6151.

recently by Armstrong of  $49.2$  kcal/mol.<sup>8</sup> Additional bond strength estimates quoted by Armstrong are  $\text{MeS-SMe} = 65.5$  and  $\text{HS-SH} = 64.5$ .

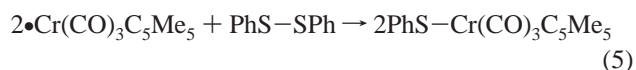
The weaker bond strength of the aryl disulfides is attributed to the stabilization of the  $\bullet\text{SPh}$  radical relative to  $\bullet\text{SR}$  radicals by delocalization in the  $\pi$  system. This stabilization energy was estimated<sup>9</sup> by Benson to be  $\sim 10$  kcal/mol, a significant decrease compared to the  $\bullet\text{OPh}$  radical where a stabilization energy of  $\sim 17$  kcal/mol was estimated. It seems reasonable to assume that this stabilization would continue to decrease while descending group 16; however, the authors could not find literature data for the estimation of the additional stabilization of the heavier congeners  $\bullet\text{SePh}$  and  $\bullet\text{TePh}$ . Theoretical calculations of the  $\text{MeSe-SeMe}$  bond strength ranging from  $30$  to  $61$  kcal/mol have been reported.<sup>10</sup> Aside from an early report for  $\text{PhSe-SePh}$ ,<sup>3</sup> experimental data for enthalpies of formation of alkyl or aryl diselenides or ditellurides could not be found.

Data for these bond strengths are important in understanding the oxidative addition reactions of transition-metal complexes and the heavier dichalcogenides. We have recently studied synthetic, kinetic, and thermodynamic aspects<sup>11</sup> of oxidative addition reactions to the metal complexes and metal-bound ligands such as those shown in eqs 3 and 4

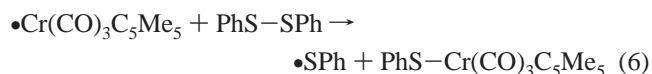


where  $\text{R} = t\text{-Bu}$  and  $\text{Ar} = 3,5\text{-C}_6\text{H}_3\text{Me}_2$ . Prior to understanding the thermochemistry of reactions of complexes of selenides and tellurides, however, it is essential to obtain relevant bond strength estimates for the main-group  $\text{PhE-EPh}$  compounds themselves.

A thermodynamic study of reaction 5 indicated that the  $\text{Cr-SPh}$  bond was  $\sim 8$  kcal/mol weaker than the  $\text{S-S}$  bond in  $\text{PhS-SPh}$ .<sup>12</sup>



Kinetic studies showed an enthalpy of activation of  $\sim 10$  kcal/mol for this reaction.<sup>12</sup> This and other observations indicated that reaction 5 occurred by rate-determining radical scission, as shown in eq 6:



The low overbarrier to reaction 6 ( $\sim 2$  kcal/mol) is in keeping with literature data for related radical reactions. Franz and co-workers have shown that  $\bullet\text{SPh}$  radicals abstract H atoms

- (8) Armstrong, D. A. In *S-Centered Radicals*; Alfassi, Z. B., Ed.; John Wiley & Sons: New York, 1999.
- (9) Benson, S. W. *Chem. Rev.* **1978**, *78*, 23.
- (10) Muang, N.; Williams, J. O.; Wright, A. C. *THEOCHEM* **1998**, *453*, 181.

from transition-metal hydrides with very low activation energies.<sup>13</sup> Organic radicals react with  $\text{H}-\text{ER}$  with enthalpies of activation of less than 2 kcal/mol.<sup>14</sup> The  $\bullet\text{SCH}_3$  radical is reported to react in the gas phase with  $\text{MeS}-\text{SMe}$  with an activation energy of  $\sim 1.5$  kcal/mol.<sup>15</sup>

In the present work, we combine kinetic and thermodynamic data to estimate the bond strengths themselves, relying on the assumption that for selenium and tellurium,  $\Delta H^\ddagger - \Delta H^\circ \approx 2$  kcal/mol for radical reactions analogous to that shown in eq 6 for sulfur. These data are extended to include an experimental estimate of the  $\text{PhSe}-\text{H}$  bond strength as well as an estimation of an upper limit for the  $\text{PhTe}-\text{H}$  bond dissociation energy (BDE). Theoretical calculations provide additional insight and are in reasonable accord with the experimental data. The crystal structures of  $\text{Ph}-\text{S}-\text{Cr}(\text{CO})_3(\eta^5\text{-C}_5\text{Me}_5)$  and  $\text{Ph}-\text{Se}-\text{Cr}(\text{CO})_3(\eta^5\text{-C}_5\text{Me}_5)$  are reported.

## Experimental Section

All preparative work and physical measurements (in particular, stopped-flow kinetic measurements) were performed under an atmosphere of purified argon using standard inert atmosphere techniques strictly analogous to those reported in previous studies.<sup>11,12</sup> The compounds  $\text{PhE}-\text{EPh}$  were obtained from Aldrich Chemical and recrystallized from a toluene/heptane solution prior to use. The complexes  $[\text{Cr}(\text{CO})_3(\eta^5\text{-C}_5\text{Me}_5)]_2$  and  $\text{H}-\text{Cr}(\text{CO})_3(\eta^5\text{-C}_5\text{Me}_5)$  were prepared and purified as described previously.<sup>11,28</sup> Infrared data were obtained in toluene solution in  $\text{CaF}_2$  cells obtained from Harrick Scientific on a Perkin-Elmer System-2000 FTIR spectrometer. UV-vis data were obtained on a Shimadzu UV-vis spectrometer of solutions loaded in quartz cells obtained from Wilmad Scientific. The cells were loaded and capped in a glovebox from freshly prepared solutions under an argon atmosphere.

### Enthalpy of Reaction of $\text{PhE}-\text{EPh}$ and $\bullet\text{Cr}(\text{CO})_3(\eta^5\text{-C}_5\text{Me}_5)$ .

A typical experimental procedure is described. In a glovebox under an argon atmosphere, a solution of 1.43 g of  $[\text{Cr}(\text{CO})_3(\eta^5\text{-C}_5\text{Me}_5)]_2$

in 210 mL of freshly distilled toluene is prepared in a Schlenk tube. This solution is filtered into a clean flask, taken from the glovebox, and loaded into the calorimeter by cannula transfer. The calorimeter system is of a special design for air sensitive work and was constructed by Ace Glass. It contains a sealed Dewar flask with six threaded glass joints as the only openings. The entire calorimeter is mounted to the rocking mechanism of an autoclave modified to give a  $180^\circ$  rotation of the entire apparatus. Once loaded, three of the six threaded joints are used to seal Teflon rods that contain sealed ampules of between 0.100 and 0.200 g of recrystallized  $\text{PhE}-\text{EPh}$ . Two of the remaining joints house a rapid response thermistor obtained from Omega Scientific and a calibrated electric heater. The final threaded joint is attached to a stopcock, which can be connected to a Schlenk line during filling or sample removal. This design allows measurement of the thermal response of breaking three ampules in sequence without opening or exposing the calorimeter to air. The rotating shaft of the autoclave rocker is fed through the wall of a thermostated chamber held at  $20^\circ\text{C}$ . The entire apparatus was calibrated first and found to be accurate on the basis of the measurement of the enthalpy of solution of tris-(hydroxymethyl) aminomethane in 0.1 N hydrochloric acid. The response time of the calorimeter system is on the order of 10 s. During operation, electrical calibrations are run before and after ampule breaking, and the calorimeter is momentarily stopped from rocking during the ampule breaking procedure. Measured data based on the reaction of the solid dichalcogenides was corrected for the enthalpy of solution of the solid dichalcogenide, which was measured separately. At the concentration and temperature of the runs, small amounts of  $[\text{Cr}(\text{CO})_3(\eta^5\text{-C}_5\text{Me}_5)]_2$  are present in solutions that are predominantly  $\bullet\text{Cr}(\text{CO})_3(\eta^5\text{-C}_5\text{Me}_5)$ . Concomitant with the reaction with dichalcogenide, a small amount of residual dimer will dissociate to a radical monomer. Reported data is the average of at least six independent measurements and is corrected using reported  $K_{\text{eq}}$  data<sup>29</sup> so that all of the species are as reported in the reaction.

**Crystal Growth of  $\text{Ph}-\text{S}-\text{Cr}(\text{CO})_3(\eta^5\text{-C}_5\text{Me}_5)$  and  $\text{Ph}-\text{Se}-\text{Cr}(\text{CO})_3(\eta^5\text{-C}_5\text{Me}_5)$ .** Following solution calorimetric measurements as described above, additional phenyl disulfide to give the correct stoichiometry to yield  $\text{Ph}-\text{S}-\text{Cr}(\text{CO})_3(\eta^5\text{-C}_5\text{Me}_5)$  was weighed into a Schlenk flask. The calorimetric solution was transferred by cannula to this flask, the solid dissolved by shaking the vessel, and the solution left at room temperature for about 2 h. Following that time, it was filtered into a clean Schlenk vessel, reduced in volume

- (11) (a) Mendriatta, A.; Cummins, C. C.; Kryatova, O. P.; Rybak-Akimova, E. V.; McDonough, J. E.; Hoff, C. D. *Inorg. Chem.* **2003**, *42*, 8621. (b) McDonough, J. E.; Wier, J. J.; Sukcharoenphon, K.; Hoff, C. D.; Kryatova, O. P.; Rybak-Akimova, E. V.; Scott, B.; Kubas, G. J.; Stephens, F. H.; Mendriatta, A.; Cummins, C. C. Manuscript in preparation.
- (12) Ju, T. D.; Capps, K. B.; Lang, R. F.; Roper, G. C.; Hoff, C. D. *Inorg. Chem.* **1997**, *36*, 614.
- (13) Franz, J. A.; Linehan, J. C.; Birnbaum, J. C.; Hicks, K. W.; Alnajjar, M. S. *J. Am. Chem. Soc.* **1999**, *121*, 9824.
- (14) (a) Newcomb, M.; Choi, S. Y.; Horner, J. H. *J. Org. Chem.* **1999**, *64*, 1225. (b) Renaud, P. *Top. Curr. Chem.* **2000**, *208*, 81.
- (15) Urbanski, S. P.; Wine, P. H. In *S-Centered Radicals*; Alfassi, Z. B., Ed.; John Wiley & Sons: New York, 1999.
- (16) te Velde, G.; Bickelhaupt, F. M.; van Gisbergen, S. J. A.; Fonseca Guerra, C.; Baerends, E. J.; Snijders, J. G.; Ziegler, T. *J. Comput. Chem.* **2001**, *22*, 931.
- (17) Fonseca Guerra, C.; Snijders, J. G.; te Velde, G.; Baerends, E. J. *Theor. Chem. Acc.* **1998**, *99*, 391.
- (18) *ADF2004.01*; Scientific Computing & Modeling: Amsterdam, The Netherlands. <http://www.scm.com>.
- (19) Vosko, S. H.; Wilk, L.; Nusair, M. *Can. J. Phys.* **1980**, *58*, 1200.
- (20) Becke, A. *Phys. Rev. A: At., Mol., Opt. Phys.* **1988**, *38*, 3098.
- (21) Perdew, J. P. *Phys. Rev. B: Condens. Matter* **1986**, *34*, 7406.
- (22) Perdew, J. P. *Phys. Rev. B: Condens. Matter* **1986**, *33*, 8822.
- (23) See, for example: Deng, L.; Schmid, R.; Ziegler, T. *Organometallics* **2000**, *19*, 3069.
- (24) van Lenthe, E.; Baerends, E. J.; Snijders, J. G. *J. Chem. Phys.* **1993**, *99*, 4597.
- (25) van Lenthe, E. The ZORA Equation. Thesis, Vrije Universiteit, Amsterdam, Netherlands, 1996.

- (26) The current data agrees, within overlap of experimental error, with earlier data reported in ref 11. The earlier enthalpy of reaction with  $\text{PhS}-\text{SPh}$  was reported as  $\Delta H = -26.6 \pm 3.0$  kcal/mol, which compares to the current value of  $\Delta H = -29.6 \pm 2.2$  kcal/mol. It is known, as described in ref 4, that the loss of CO and formation of dinuclear S-bridged complexes are endothermic for analogous complexes of Mo. Despite the overlap, the current measured value is considered more accurate because the earlier measurement was made at a higher temperature and over a 1–2 h time period, which may have allowed the dinuclear complex to be formed in an amount too small to be detected spectroscopically. As a result of the highly air-sensitive nature of the radical, however, it may simply be that the independent measurements reflect the statistical error in the measurement process. Because one goal of this work was a side-by-side comparison of the S, Se, and Te derivatives, it was deemed necessary to repeat this measurement.
- (27) (a) Goh, L. Y.; Tay, M. S.; Mak, T. C. W.; Wang, R. J. *Organometallics* **1992**, *11*, 1711. (b) Goh, L. Y.; Tay, M. S.; Wei, C. *Organometallics* **1994**, *13*, 1813. (c) Goh, L. Y.; Lim, Y. Y.; Tay, M. S.; Mak, T. C. W.; Zhou, Z. Y. *J. Chem. Soc., Dalton Trans.* **1992**, 1239.
- (28) Sukcharoenphon, K.; Moran, D.; Schleyer, P. V. R.; McDonough, J. E.; Abboud, K. A.; Hoff, C. D. *Inorg. Chem.* **2003**, *42*, 8494.
- (29) Watkins, W. C.; Jaeger, T.; Kidd, C. E.; Fortier, S.; Bard, M. C.; Kiss, G.; Roper, G. C.; Hoff, C. D. *J. Am. Chem. Soc.* **1992**, *114*, 907.

from approximately 200 mL to approximately 50 mL, and placed in the freezer. Over a period of 1 month, dark red crystals of Ph–S–Cr(CO)<sub>3</sub>(η<sup>5</sup>-C<sub>5</sub>Me<sub>5</sub>) formed in the flask and were isolated. Similar procedures were used to prepare Ph–Se–Cr(CO)<sub>3</sub>(η<sup>5</sup>-C<sub>5</sub>Me<sub>5</sub>). Full structural data are reported in the Supporting Information.

**Reaction of PhSe–SePh and PhTe–TePh with H–Cr(CO)<sub>3</sub>(η<sup>5</sup>-C<sub>5</sub>Me<sub>5</sub>).** In a glovebox, a solution of 0.06 g of [Cr(CO)<sub>3</sub>(η<sup>5</sup>-C<sub>5</sub>Me<sub>5</sub>)<sub>2</sub>] was prepared in 3 mL of C<sub>6</sub>D<sub>6</sub>. This was then stirred under 1.5 atm of H<sub>2</sub> for 2 h to produce a solution of H–Cr(CO)<sub>3</sub>(η<sup>5</sup>-C<sub>5</sub>Me<sub>5</sub>). To this solution was added a solution of 0.07 g of PhSe–SePh in 2 mL of C<sub>6</sub>D<sub>6</sub>. A FTIR spectrum run within twenty seconds of the addition showed a complete conversion to Ph–Se–Cr(CO)<sub>3</sub>(η<sup>5</sup>-C<sub>5</sub>Me<sub>5</sub>). NMR data showed the formation of H–SePh. Reactions done in an analogous fashion with PhTe–TePh showed no reaction over a period of 1 h. The addition of ~10 mol % •Cr(CO)<sub>3</sub>(η<sup>5</sup>-C<sub>5</sub>Me<sub>5</sub>) resulted in the stoichiometric conversion of the radical complex to Ph–Te–Cr(CO)<sub>3</sub>(η<sup>5</sup>-C<sub>5</sub>Me<sub>5</sub>) but no conversion of H–Cr(CO)<sub>3</sub>(η<sup>5</sup>-C<sub>5</sub>Me<sub>5</sub>) over an additional 1 h time period.

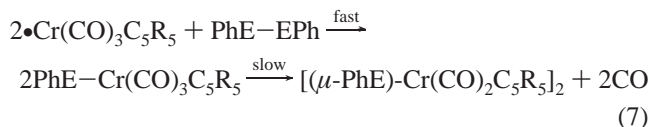
**Computational Details.** All density functional theory (DFT) calculations were carried out using the Amsterdam Density Functional (ADF) program package,<sup>16,17</sup> version 2004.01.<sup>18</sup> The local exchange-correlation potential of Vosko et al.<sup>19</sup> (VWN) was augmented self-consistently with gradient-corrected functionals for electron exchange according to Becke<sup>20</sup> and for electron correlation according to Perdew.<sup>21,22</sup> This nonlocal density functional is termed BP86 in the literature and has been shown to give excellent results for both the geometries and energetics of transition-metal systems.<sup>23</sup> Relativistic effects were included using the zero-order regular approximation (ZORA).<sup>24,25</sup> The basis set used was the all-electron ADF ZORA/TZ2P (triple ζ with two polarization functions) basis.

**Stopped-Flow and UV–Vis Study of Reactions.** Stopped-flow kinetic studies were done using a Hi-Tech Scientific (Salisbury, Wiltshire, U.K.) SF-43 Multi-Mixing CryoStopped-Flow instrument equipped with stainless steel plumbing, a stainless steel mixing cell with sapphire windows, and an anaerobic gas-flushing kit. The instrument was connected to an IBM computer with IS-2 Rapid Kinetics software by Hi-Tech Scientific. The temperature in the mixing cell was maintained to ±0.1 K, and the mixing time of the instrument is 2 ms. Time-resolved spectra were acquired with a diode array attachment. Because of the relatively rapid nature of the reactions, a pseudo-first-order study of the reactions of •Cr(CO)<sub>3</sub>C<sub>5</sub>Me<sub>5</sub> and PhE–EPh was not attempted. In a typical procedure, solutions that, prior to mixing, were exactly matched and equal to 1 mM concentrations of [Cr(CO)<sub>3</sub>C<sub>5</sub>R<sub>5</sub>]<sub>2</sub> and PhE–EPh were prepared in toluene under strictly anaerobic conditions in a glovebox, loaded into gastight syringes equipped with three-way valves, and then transferred to the stopped-flow system, which was purged with argon. Upon mixing, these solutions are diluted to 0.5 mM, and at temperatures above 10 °C, the concentration of the radical monomer •Cr(CO)<sub>3</sub>C<sub>5</sub>Me<sub>5</sub> corresponds to >94% of the total Cr concentration, as calculated on the basis of published data.<sup>28</sup> Dissociation of the Cr–Cr dimer is rapid<sup>33</sup> compared to all of the other reactions studied, and the absorption spectrum of the dimer

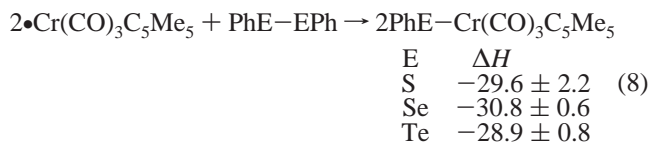
was found to not significantly interfere with kinetic studies at temperatures above 10 °C. Additional information as well as spectroscopic and kinetic data are provided as supporting information.

## Results and Discussion

**Reaction of •Cr(CO)<sub>3</sub>C<sub>5</sub>Me<sub>5</sub> and PhE–EPh.** Reactions of •Cr(CO)<sub>3</sub>C<sub>5</sub>R<sub>5</sub> (R = H, CH<sub>3</sub>) and dichalcogenides have been extensively studied from a synthetic point of view. The initially formed PhE–Cr(CO)<sub>3</sub>C<sub>5</sub>R<sub>5</sub> adduct is known to lose CO and form dimeric chalcogen-bridged complexes:



Because of the fact that slow formation of these dimers occurs, calorimetric measurements were performed using a more rapid response isoperibol calorimeter as opposed to the Calvet techniques used originally on the reaction of PhS–SPh.<sup>26</sup> To compare data on all dichalcogenides under the same conditions, the PhS–SPh measurements were repeated using this method as well. Experimental data in eq 8 refers to the enthalpy of reaction with all of the components in toluene solution as shown.



The measured enthalpies of reaction are remarkably constant for reaction 8 and imply that changes in the PhE–EPh bond strength are roughly 1/2 the changes in the PhE–Cr bond as a function of E throughout this series.

**Structures of PhE–Cr(CO)<sub>3</sub>C<sub>5</sub>Me<sub>5</sub> for E = S, Se. Are There Signs of Steric Strain in the Cr–EPh Bond?** The crystal structures of the derivatives where R = H and E = Se and Te have been reported by Goh and co-workers,<sup>27</sup> whereas for the E = S derivatives, only bridged dimers such as [(μ-PhS)–Cr(CO)<sub>2</sub>C<sub>5</sub>H<sub>5</sub>]<sub>2</sub> have been structurally characterized. As part of an investigation of pyridine thione reactivity, we recently reported<sup>28</sup> the structures of (η<sup>2</sup>-2-mp)–Cr(CO)<sub>2</sub>C<sub>5</sub>Me<sub>5</sub> and (η<sup>1</sup>-4-mp)–Cr(CO)<sub>3</sub>C<sub>5</sub>Me<sub>5</sub>. Following solution calorimetric studies performed in this work, we obtained X-ray quality crystals of PhS–Cr(CO)<sub>3</sub>C<sub>5</sub>Me<sub>5</sub> and PhSe–Cr(CO)<sub>3</sub>C<sub>5</sub>Me<sub>5</sub> and determined their structures. Complete structural details are available as supporting information. Figure 1 shows an overlay of the two “piano stool” structures for the isostructural S and Se derivatives. It might be expected that in going from the Se to S derivative that the shorter Cr–S bond length might result in some distortion of the CO or Cp\* ligands away from the E–Ph group. There is no sign of that occurring, and little ligand rearrangement around Cr is found in changing from S to Se. A lengthening of the Cr–EPh bond from 2.4526 Å (E = S) to 2.5890 Å

(30) Adams, R. D.; Collins, D. E.; Cotton, F. A. *J. Am. Chem. Soc.* **1974**, *96*, 749.

(31) McClain, S. L. *J. Am. Chem. Soc.* **1988**, *110*, 643.

(32) Yao, Q.; Bakac, A.; Espenson, J. H. *Organometallics* **1993**, *12*, 2010.

(33) Richards, T. C.; Geiger, W. E.; Baird, M. C. *Organometallics* **1994**, *13*, 4494.

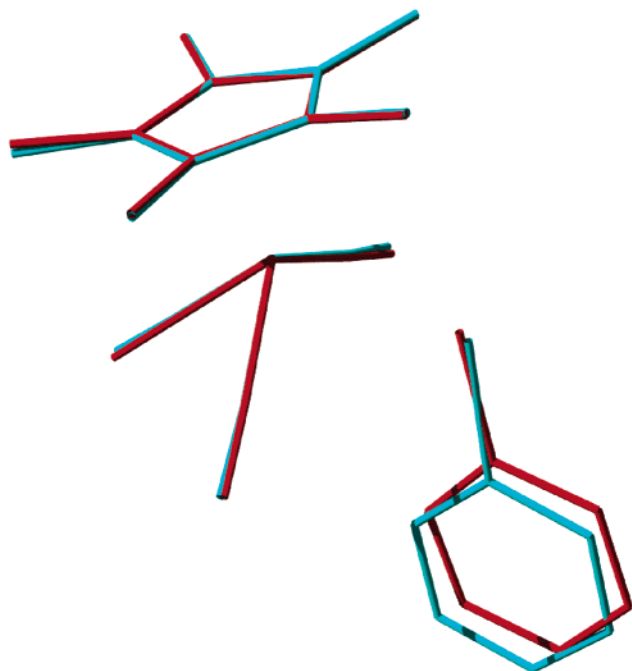
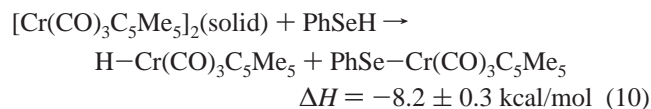
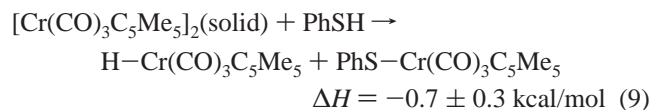


**Figure 1.** Overlay of  $\text{PhS}-\text{Cr}(\text{CO})_3\text{C}_5\text{Me}_5$  (red) and  $\text{PhSe}-\text{Cr}(\text{CO})_3\text{C}_5\text{Me}_5$  (turquoise) structures showing little distortion of ancillary metal–ligand bonds. The  $\text{Cr}-\text{EPh}$  bond vector is omitted for clarity. Separated structural pictures and full crystallographic data are available in the Supporting Information.

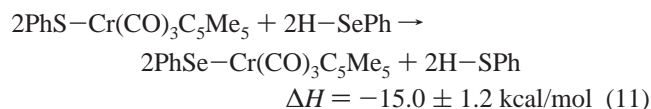
( $\text{E} = \text{Se}$ ) and a narrowing of the  $\text{Cr}-\text{E}-\text{Ph}$  bond angle from  $114.44^\circ$  ( $\text{E} = \text{S}$ ) to  $109.85^\circ$  ( $\text{E} = \text{Se}$ ) are the dominant structural differences.

It is also worth noting that the  $\text{Cr}-\text{SePh}$  bond length for  $\text{PhSe}-\text{Cr}(\text{CO})_3\text{C}_5\text{Me}_5$  (2.5890) reported here is essentially the same as that reported earlier by Goh for  $\text{PhSe}-\text{Cr}(\text{CO})_3\text{C}_5\text{H}_5$  (2.588).<sup>27</sup> That is in contrast to the metal–metal bonded dimers  $(\text{C}_5\text{R}_5)(\text{CO})_3\text{Cr}-\text{Cr}(\text{CO})_3(\text{C}_5\text{R}_5)$  where the  $\text{Cr}-\text{Cr}$  bond is longer for  $\text{R} = \text{CH}_3$ <sup>29</sup> (3.3107 Å) than for  $\text{R} = \text{H}$ <sup>30</sup> (3.288 Å). This also implies no significant change in steric factors in going from S to Se in these complexes.

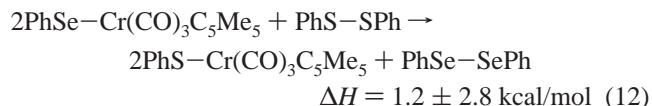
**The Enthalpy of Hydrogenation of  $\text{PhSe}-\text{SePh}$ .** Enthalpy of hydrogenation data can provide a valuable method to estimate element–hydride bond strengths. Two approaches to determine this were used for  $\text{PhSeH}$ . The first is based on measurements of eqs 9 and 10:



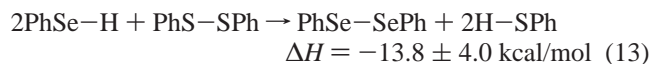
The subtraction of twice eq 9 from twice eq 10 yields eq 11:



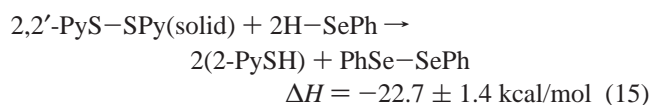
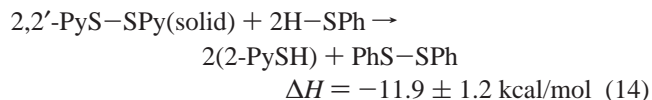
Data from eq 8 can be used to calculate the enthalpy of eq 12:



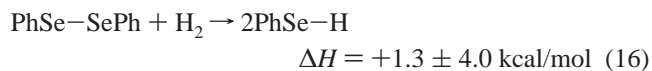
Addition of eqs 11 and 12 leads to a calculated enthalpy of reaction 13:



A second method is based on the enthalpy of reaction of 2,2' pyridine disulfide, as shown in eqs 14 and 15:

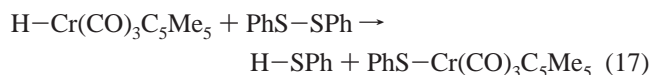


Subtraction of eq 14 from eq 15 leads to an independent measurement of reaction 13 and yields a value of  $\Delta H = -10.8 \pm 2.6 \text{ kcal/mol}$ . An average value of  $\Delta H = -12.3 \pm 4.0 \text{ kcal/mol}$  appears to be a reasonable value for reaction 13 based on these two independent methods. It should be emphasized that the measured enthalpies leading to this estimate each combine several measured enthalpies, all of which are for rather difficult reactions. Because the enthalpy of hydrogenation of phenyl disulfide in toluene solution is  $-11 \text{ kcal/mol}$ , it is, therefore, straightforward to conclude that

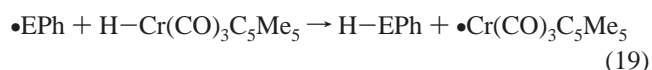
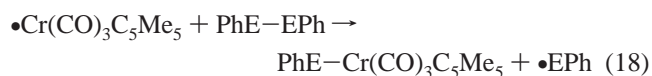


Using the estimate for  $\text{PhSe}-\text{SePh}$  of 41 kcal/mol derived below yields a first estimate of  $\text{PhSe}-\text{H}$  of  $72 \pm 3 \text{ kcal/mol}$ .

**Reaction of  $\text{H}-\text{Cr}(\text{CO})_3\text{C}_5\text{Me}_5/\bullet\text{Cr}(\text{CO})_3\text{C}_5\text{Me}_5$  and  $\text{PhE}-\text{EPh}$ .** In earlier work,<sup>12</sup> we had investigated the reaction of phenyl disulfide with the chromium hydride complex, as shown in eq 17:



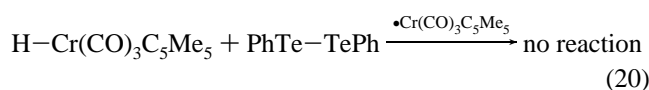
The rate of reaction 17 was found to depend greatly on the amount of residual radical present in the hydride solution. The two-step radical chain mechanism shown in eqs 18 and 19 was shown to operate for  $\text{E} = \text{S}$ .



These earlier studies were extended to the heavier dichalcogenides.

In the case of PhSe–SePh, rapid and quantitative oxidative addition of H–Cr(CO)<sub>3</sub>C<sub>5</sub>Me<sub>5</sub> occurred in the presence of only trace amounts of •Cr(CO)<sub>3</sub>C<sub>5</sub>Me<sub>5</sub>. The rapid nature of the reaction of phenyl diselenide is in keeping with a radical chain mechanism similar to that observed earlier for PhS–SPh. A key aspect of this radical chain reaction is eq 19, in which in situ •EPh must be competent to abstract an H atom from H–Cr(CO)<sub>3</sub>C<sub>5</sub>Me<sub>5</sub> to continue the chain. As discussed above, thermodynamic data indicate the H–SePh bond enthalpy to be ~72 kcal/mol as compared with the Cr–H bond enthalpy of ~63 kcal/mol; thus, reaction 19 is both thermodynamically favored and expected to have a low enthalpy of activation, allowing the chain reaction of 18 and 19 to occur rapidly.

In contrast, attempts to study analogous reaction chemistry with PhTe–TePh showed no reaction over a 2 h period, even when the chromium radical was deliberately injected into the reaction solution:



The failure of reaction 20 to proceed to the right implies that either reaction 18 or reaction 19 is not competent for E = Te. As we will discuss later, the attack of the chromium radical on the (reaction 18) is even faster for Te than it is for Se, and so it must be H atom transfer (reaction 19) that is responsible for the failure of reaction 20 to proceed as written. Because kinetic barriers for such a H atom transfer are low, this implies that the PhTe–H bond strength is ≤ 63 kcal/mol.

**UV–Vis Spectroscopy of •Cr(CO)<sub>3</sub>C<sub>5</sub>Me<sub>5</sub>, PhE–Cr(CO)<sub>3</sub>C<sub>5</sub>Me<sub>5</sub>, and PhE–EPh.** A qualitative kinetic study of the rates of reactions 7 and 8 by FTIR indicated that they were too rapid to be studied by the same techniques employed for PhS–SPh<sup>12</sup> and that stopped-flow kinetics would be needed to obtain quantitative data. Prior to these studies, it was necessary to investigate the UV–vis spectroscopy of these species, in particular that of •Cr(CO)<sub>3</sub>C<sub>5</sub>Me<sub>5</sub>, which exists in rapid equilibrium with its dimer,<sup>29</sup> as shown in eq 21:



UV–vis spectral data (Figure SI-1, Supporting Information) as well as stopped-flow kinetic spectral data, discussed later, support that although the metal–metal bonded dimer has a strong  $\lambda_{\text{max}}$  near 465 nm, the radical complex •Cr(CO)<sub>3</sub>C<sub>5</sub>Me<sub>5</sub> shows only a weak absorption, which is a broad band from 450 to 600 nm. These results are qualitatively similar to the spectral data reported by McClain<sup>31</sup> for the related but less extensively dissociated radical/dimer pair •Cr(CO)<sub>3</sub>C<sub>5</sub>H<sub>5</sub>/C<sub>5</sub>H<sub>5</sub>(CO)<sub>3</sub>Cr–Cr(CO)<sub>3</sub>C<sub>5</sub>H<sub>5</sub>. For •Cr(CO)<sub>3</sub>C<sub>5</sub>Me<sub>5</sub>/C<sub>5</sub>Me<sub>5</sub>(CO)<sub>3</sub>Cr–Cr(CO)<sub>3</sub>C<sub>5</sub>Me<sub>5</sub>, a strong peak with  $\lambda_{\text{max}}$  at 512 nm has been reported in the literature<sup>32</sup> and was assigned to [Cr(CO)<sub>3</sub>C<sub>5</sub>Me<sub>5</sub>]<sub>2</sub>. However, under anaerobic conditions, no such absorption was seen in our work. The deliberate injection of air into a solution of •Cr(CO)<sub>3</sub>C<sub>5</sub>Me<sub>5</sub> results in

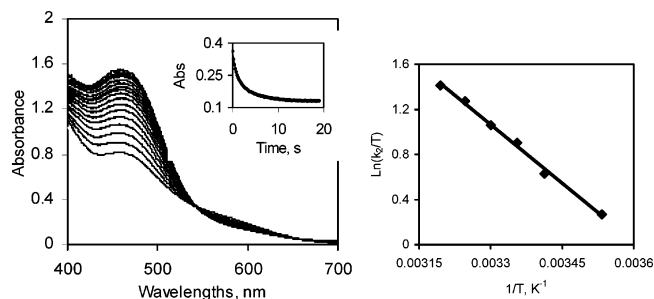


**Figure 2.** Time-resolved (20 s scan, 1 s intervals) spectral changes and a kinetic trace at 600 nm (overlapped with a second-order fit) obtained upon mixing toluene solutions of [Cr(CO)<sub>3</sub>C<sub>5</sub>Me<sub>5</sub>]<sub>2</sub> (1 mM) and Ph<sub>2</sub>Se<sub>2</sub> (1 mM) in a stopped-flow cell at 10 °C. An Eyring equation plot yielding activation parameters  $\Delta H^\ddagger = 7.0 \pm 0.5$  kcal/mol and  $\Delta S^\ddagger = -22 \pm 3$  eu ( $R^2 = 0.996$ ) is also shown.

the formation of a meta-stable, blood-red adduct between oxygen and •Cr(CO)<sub>3</sub>C<sub>5</sub>Me<sub>5</sub> with  $\lambda_{\text{max}}$  at 512 nm (Figure SI-2, Supporting Information). It seems likely that the literature data<sup>32</sup> analysis based on the monitoring of the peak at  $\lambda_{\text{max}} = 512$  nm corresponded to the oxygen adduct and not the radical. That could explain the apparent disagreement between rate constants derived for this radical and the same rate constants derived by the electrochemical results of Baird and co-workers.<sup>33</sup>

Selection of the spectral window to study was also dictated by the UV–vis spectrum of the dichalcogenides and their complexes (Figures SI-3 and SI-4, Supporting Information). Of particular note is the need to avoid photochemical activation and radical formation of the dichalcogenides themselves, which change from white (PhS–SPh) to yellow (PhSe–SePh) to orange (PhTe–TePh). In addition, it is well-known that the product complexes are photolabile. For example, Abrahamson and co-workers<sup>34</sup> have shown that a loss of CO and a subsequent reactivity or dimerization occurs photochemically for ArS–W(CO)<sub>3</sub>C<sub>5</sub>H<sub>5</sub> complexes at 436 nm. The product complexes PhE–Cr(CO)<sub>3</sub>C<sub>5</sub>Me<sub>5</sub> were found to have absorptions in this area, which trail off to higher wavelengths (Figure SI-4, Supporting Information). On the basis of these observations, the majority of the reactions were followed by monitoring the band at 550 nm for decay of the radical. Reactions were performed in both single wavelength and diode array modes (the latter allows time-resolved spectra to be acquired). In some cases, as described below, decomposition attributed to secondary photochemistry was observed when either high-energy light was employed or monitoring was performed for long reaction times. In these cases, single wavelength monitoring of the reaction was followed.

**Stopped-Flow Kinetic Studies. Reaction of •Cr(CO)<sub>3</sub>C<sub>5</sub>Me<sub>5</sub> and PhSe–SePh.** This reaction was studied under conditions of matched stoichiometry between the reactants. Typical kinetic data as well as an Eyring plot for the reaction of PhSe–SePh with •Cr(CO)<sub>3</sub>C<sub>5</sub>Me<sub>5</sub> are shown in Figure 2.

(34) (a) Weinman, D. J.; Abrahamson, H. B. *Inorg. Chem.* **1987**, *26*, 2133. (b) Brandenburg, K. L.; Heeg, M. J.; Abrahamson, H. B. *Inorg. Chem.* **1987**, *26*, 1064.

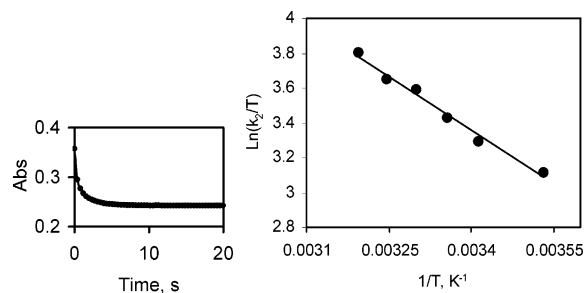


**Figure 3.** Kinetic trace at 550 nm obtained upon mixing toluene solutions of  $[\text{Cr}(\text{CO})_3\text{C}_5\text{Me}_5]_2$  (1 mM) and  $\text{Ph}_2\text{Te}_2$  (1 mM) in a stopped-flow cell at 10 °C using a visible spectrum lamp at the single wavelength mode. No photochemical decomposition was observed under these conditions. A plot of the temperature dependence of the second-order rate constant for the reaction of  $[\text{Cr}(\text{CO})_3\text{C}_5\text{Me}_5]_2$  (1 mM) and  $\text{Ph}_2\text{Te}_2$  (1 mM) in toluene is also shown. The fit to the linear form of the Eyring equation gives activation parameters of  $\Delta H^\ddagger = 4.0 \pm 0.5$  kcal/mol and  $\Delta S^\ddagger = -26 \pm 3$  eu ( $R^2 = 0.99$ ).

These data led to reproducible kinetics under all conditions on a short time scale. When studied with polychromatic light, however, photochemistry was observed leading to the decomposition of  $\text{PhSe}-\text{Cr}(\text{CO})_3\text{C}_5\text{Me}_5$  (Figure SI-5, Supporting Information). This did not interfere with the kinetic runs. A study of this reaction by FTIR spectroscopy in the absence of light showed that  $\text{PhSe}-\text{Cr}(\text{CO})_3\text{C}_5\text{Me}_5$  is formed rapidly and quantitatively and does not decompose in the dark over time scales longer than those used in the stopped-flow experiments. A photochemical loss of CO, as observed earlier by Abrahamson et al.<sup>34</sup> for analogous W complexes, is proposed to occur in the stopped-flow cell.

**Reaction of  $\bullet\text{Cr}(\text{CO})_3\text{C}_5\text{Me}_5$  and  $\text{PhTe}-\text{TePh}$ .** The rather slow photodecomposition of  $\text{PhSe}-\text{Cr}(\text{CO})_3\text{C}_5\text{Me}_5$  referred to in the preceding section was found to be much more significant for  $\text{PhTe}-\text{Cr}(\text{CO})_3\text{C}_5\text{Me}_5$  (Figure SI-6, Supporting Information); a net increase in absorbance was observed when the sample was exposed to polychromatic light and, in this case, did influence the stopped-flow kinetic studies. Because of instability under these conditions, the reaction of  $\text{PhTe}-\text{TePh}$  was studied at the single wavelength mode at 550 nm. As shown in Figure 3, this allowed stable kinetic traces, which could be fit accurately to a second-order kinetic mechanism over the entire temperature range studied.

Complete data from these studies, together with those reported earlier for  $\text{PhS}-\text{SPh}$  (as well as the bond strength estimates discussed later), are summarized in Table 1.

**Combined Reaction Profile for the Oxidative Addition of  $\text{PhE}-\text{EPh}$ .** The kinetic and thermodynamic data for the oxidative addition of the dichalcogenides provide a basis for the estimation of both the  $\text{PhE}-\text{EPh}$  and  $\text{PhE}-\text{Cr}$  bond strengths. This only requires the assumption of a low overbarrier for these reactions. Data reported earlier by us on phenyl disulfide<sup>12</sup> were in agreement with that assumption, and there is considerable literature precedent in that regard.<sup>13–15</sup> Data on enthalpies of the oxidative addition of the dichalcogenides in toluene solution obey the relationship  $\Delta H_{\text{rxn}} = D_{\text{PhE}-\text{EPh}} - 2D_{\text{PhE}-\text{Cr}}$ , where it is understood that the bond dissociation energies and all of the data refer to toluene

**Table 1.** Second-Order Rate Constants,<sup>a</sup> Activation Parameters,<sup>b</sup> Enthalpies of Reaction, and Estimated Bond Strength Data<sup>c</sup> for Reactions of  $\text{PhE}-\text{EPh}$  and  $\bullet\text{Cr}(\text{CO})_3\text{C}_5\text{Me}_5$

E	<i>k</i>	$\Delta H^\ddagger$	$\Delta S^\ddagger$	$\Delta H_{\text{rxn}}$	$\text{PhE}-\text{EPh}$	$\text{PhE}-\text{Cr}$
S	1.3	10.2	-24.4	-29.6	46	38
Se	1400	7.0	-22	-30.8	41	36
Te	19000	4.0	-26	-28.9	33	31

<sup>a</sup> Rate constants are extrapolated to 298 K from activation parameters and are in  $\text{M}^{-1}\text{s}^{-1}$ . <sup>b</sup> Enthalpy of activation in kcal/mol and entropy of activation in cal/mol K. Data for S is taken from ref 12. <sup>c</sup> Bond strength estimates (kcal/mol) are in toluene solution and were generated as discussed in the text. Error limits on absolute bond strengths are in the range  $\pm 3$  kcal/mol.

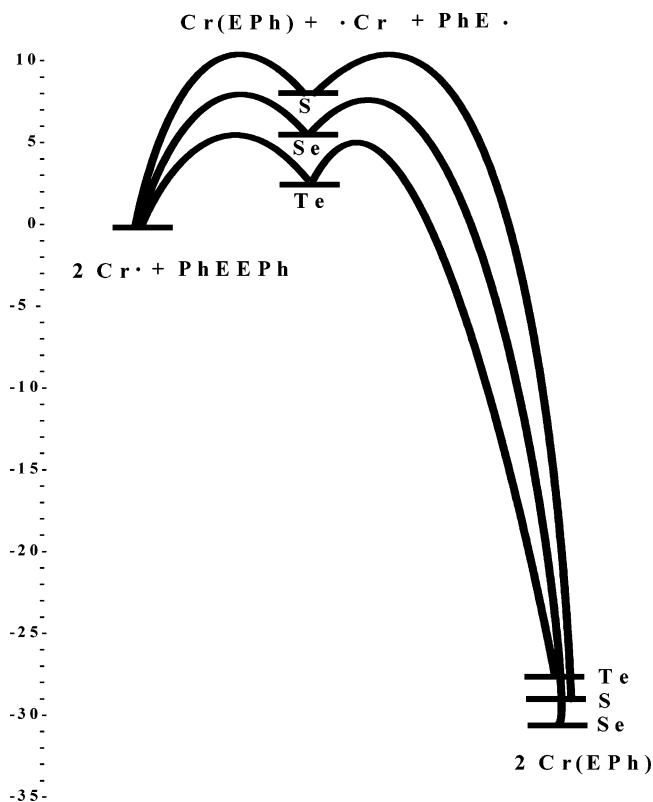


**Figure 4.** Reaction profile for the two-step cleavage of  $\text{PhE}-\text{EPh}$  by  $\bullet\text{Cr}$ . The first step corresponds to the formation of  $\text{PhE}-\text{Cr}$  and  $\bullet\text{EPh}$ , and the second step corresponds to the combination of  $\bullet\text{EPh}$  and  $\bullet\text{Cr}$ . An overbarrier of  $2 \pm 1$  kcal/mol is assumed for step i, as discussed in the text. A lower barrier of  $1.5 \pm 1$  kcal/mol is assumed for the radical combination in step ii.

solution. Assuming a low overbarrier of  $2 \pm 1$  kcal/mol in which the metallo radical attacks the dichalcogenide means that  $\Delta H^\ddagger = D_{\text{PhE}-\text{EPh}} - D_{\text{PhE}-\text{Cr}} + 2$ . These two equations allow the calculation of bond strengths based as collected in Table 1, which are used to construct the reaction profile shown in Figure 4.

**Factors Influencing the  $\text{PhE}-\text{Cr}(\text{CO})_3(\text{C}_5\text{Me}_5)$  Bond Strength.** An examination of the data in Table 1 shows that although both the  $\text{PhE}-\text{EPh}$  and  $\text{PhE}-\text{Cr}$  bonds show the expected decrease in bond strength in going from S to Se to Te, this is somewhat attenuated for the chalcogenide-metal bond strengths. Thus, the ratio of  $D_{\text{PhE}-\text{EPh}}/D_{\text{PhE}-\text{Cr}}$  goes from 0.83 (S) to 0.88 (Se) to 0.94 (Te). One possible explanation would be that, for steric reasons, the smaller  $-\text{SPh}$  group could not come into its favored bonding distance as a result

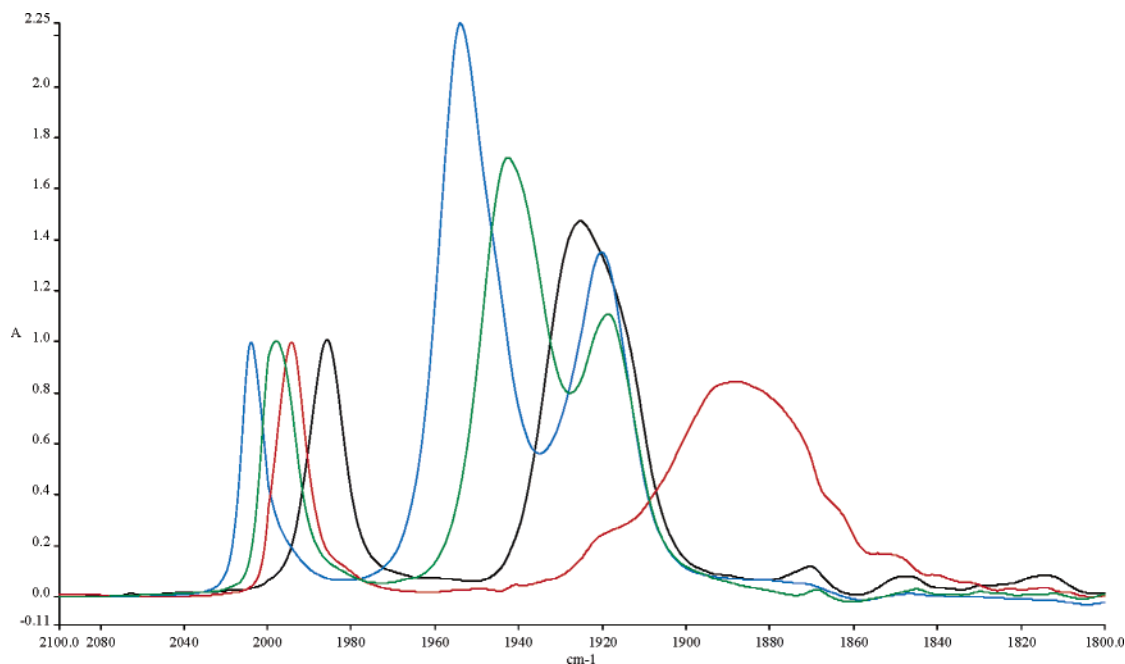


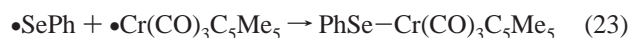
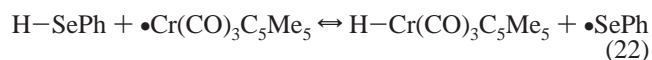
**Figure 5.** FTIR data in toluene for  $\bullet\text{Cr}(\text{CO})_3\text{C}_5\text{Me}_5$  (red) and  $\text{PhE-Cr}(\text{CO})_3\text{C}_5\text{Me}_5$  [E = S (blue), Se (green), Te (black)], showing that while oxidation moves the M–CO bands to higher wavenumbers, it does so in the order  $\text{S} > \text{Se} > \text{Te}$ .

of interligand repulsion and that, for the larger chalcogenides, this steric repulsion is not a factor. However, as shown in Figure 1, X-ray data give no indication of steric “pressure” changing, at least for the S and Se derivatives. Bond strengths in a transition-metal complex depend not only on the M–X bond but on how this bond influences the ancillary M–L bonds. In the case of metal–carbonyls, oxidation of the metal is well-known to decrease the M–CO bond strength. As shown in the FTIR data in Figure 5, following oxidation by the dichalcogenides, the E band of the tricarbonyl moves to higher wavenumbers and is split to varying degrees. The A band is also moved to higher wavenumbers for S, but less so for Se, and it actually moves to lower wavenumbers for the Te derivative. This effect is well-known in metal–carbonyl chemistry, and the degree of back bonding and, hence, the M–CO bond strength itself is perturbed by the M–X bond. On the basis of the FTIR data, the M–CO bonds would be strongest for the Cr–TePh derivative and weakest for the Cr–SPh bond. This opposing trend may explain why there is a slower rate of decrease in bond strength in the M–EPh bond versus that of the H–EPh bond for these complexes.

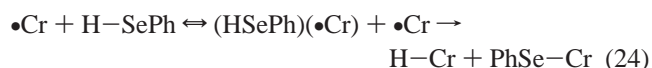
In addition, these differences in relative bond strengths for PhE–EPh and PhE–Cr result in the nearly constant enthalpy of oxidative addition in this series, as shown in the energy diagram in Figure 2. Studies of enthalpies of oxidative addition and derived bond strength data for the complexes in reaction 3, which do not contain carbonyl ligands, do not show this trend.<sup>10</sup>

**Stopped-Flow Kinetic Study of Reaction of  $\bullet\text{Cr}(\text{CO})_3\text{C}_5\text{Me}_5$  and H–SePh.** Two possible reaction mechanisms for the reaction of the chromium radical and benzeneselenol (eq 10) were considered. The first would involve the thermodynamically uphill H atom transfer reaction shown

in eq 22 followed by the radical combination reaction shown in eq 23:



The competing mechanism would be an overall third-order process, such as the one shown in eq 24:



The order of bond strengths plays a vital role in determining which of these two mechanisms is followed: [ $\text{H-Cr}$  ( $\sim 63$  kcal/mol) <  $\text{H-SePh}$  ( $\sim 72$  kcal/mol) <  $\text{H-SR}$  ( $\sim 79$ – $89$  kcal/mol)].<sup>35</sup> For both alkyl and aryl thiols, an overall third-order rate law was followed:  $d[\text{P}]/dt = k_{\text{third}}[\text{RSH}][\bullet\text{Cr}]^2$  with  $\Delta H^\ddagger \approx 0$  kcal/mol<sup>-1</sup> and  $\Delta S^\ddagger \approx -50$  cal/mol K.

The large negative entropy of activation is due to the formation of a termolecular transition state. The  $\sim 9$  kcal/mol gap in bond strengths between H–Cr and H–SePh indicates that, particularly at higher temperatures, a mechanism according to reactions 22 and 23 might be expected to compete with that in eq 24.

An initial study of the reaction of  $\bullet\text{Cr}$  with benzeneselenol showed it to be qualitatively much faster than that observed for thiophenol in infrared studies. The reaction is clean, and as described earlier, calorimetric data could be obtained. Because of the fact that benzeneselenol has no significant absorption in the spectral window and no photochemistry at these wavelengths, rate studies were done under pseudo-first-order conditions of a constant excess benzeneselenol concentration.

(35) Hoff, C. D. *Coord. Chem. Rev.* **2000**, *206*, 451.

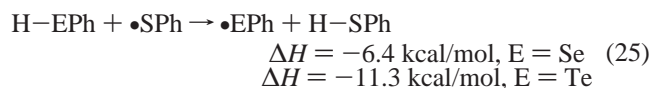


Time-resolved spectroscopic data for this reaction from  $-20$  to  $+60$  °C were obtained. Because of the spectroscopic presence of the Cr–Cr dimer, only data obtained above  $10$  °C are considered for kinetics. The data between  $-20$  and  $+10$  °C did, however, confirm the UV–vis assignment of the Cr–Cr dimer band as discussed in an earlier section. An analysis of the original spectroscopic traces at  $T = 10$ – $60$  °C showed that, in the range of  $10$ – $30$  °C, there was very little change in the apparent rate of reaction but, from  $40$ – $60$  °C, the initial rate of reaction increased (Figure SI-7, Supporting Information). The temperature-insensitive nature of the data at  $10$ ,  $20$ , and  $30$  °C recalled the data observed for the third-order activation of thiophenol, which also shows no temperature dependence on the rate.<sup>24</sup> Reasonable fits to a second-order dependence in the Cr radical could be obtained in the temperature range  $10$ – $30$  °C for an overall third-order reaction (Figure SI-8, Supporting Information). Estimates of the third-order rate constant based on these data are  $k_{\text{obs}} \approx 3900 \text{ M}^{-2}\text{s}^{-1}$ . That compares to the previously reported third-order rate constants for the reaction of the chromium radical and PhSH,  $k_{\text{obs}} \approx 25 \text{ M}^{-2}\text{s}^{-1}$ . Because the temperature dependence is low, this must be primarily due to a reduction in the entropy of activation for the reaction of benzeneselenol, by  $\sim R \ln[3900/25] \approx 10 \text{ cal/mol K}$ , in comparison to that of PhSH, for which  $\Delta S^\ddagger \approx -52 \text{ cal/mol deg}$  was determined.<sup>35</sup>

Consistent with a crossover in mechanism from third order to second order at higher temperatures, plots of  $\ln[\text{A}]$  versus time were found to be curved at  $10$ – $30$  °C but they begin to approach linearity at  $40$  °C and can be fit with straight lines at  $50$  and  $60$  °C (Figure SI-9, Supporting Information). That is consistent with the overall second-order process having a higher activation energy and overtaking the slower third-order process at the higher temperatures used. Second-order rate constants of  $7.2 \text{ M}^{-1}\text{s}^{-1}$  at  $T = 50$  °C and  $12.7 \text{ M}^{-1}\text{s}^{-1}$  at  $T = 60$  °C lead to an estimated activation energy of  $12 \text{ kcal/mol}$ , in excellent agreement with an endothermic first step calculated to be  $\sim 9 \text{ kcal/mol}$  uphill, based on the bond strength data discussed above, and calculated to have a small overbarrier to H atom transfer. These data provide additional confirmation of our assignment of the H–SePh bond strength as being  $72 \pm 3 \text{ kcal/mol}$ .

**Computational Studies.** The goals of the theoretical calculations were to investigate relative PhE–H and PhE–EPh bond strengths as well as the nature of the singly occupied molecular orbital (SOMO) for the  $\bullet\text{EPh}$  radicals. In the PAC study of the PhS–H bond strength discussed earlier,<sup>6</sup> several levels of theory were used to determine this bond strength. Composite ab initio procedures G3(MP2) led to a value of  $82.9 \text{ kcal/mol}$ , in excellent agreement with the experimental PAC studies.

DFT calculations in our work were obtained as described in more detail in the Experimental Section and used to calculate the enthalpies of reaction 25:



Because a minimum amount of correction for zero-point energy effects is anticipated, data for the nearly isodesmic reaction 25 do not include corrections for zero-point energy and are not corrected to  $298 \text{ K}$ .<sup>36</sup> In the case of the open-shell systems, calculations were carried out using the spin-unrestricted formalism. The values of  $S^2$  (exact, expectation value) calculated for these radicals were: SPh, (0.750 00, 0.758 60); SePh (0.750 00, 0.756 00); TePh (0.750 00, 0.754 16).<sup>37</sup>

Using a value for the PhS–H bond strength in toluene solution of  $81 \pm 3 \text{ kcal/mol}$  (as discussed in ref 6b) and assuming negligible solvation energy effects for reaction 25 leads to a theoretical estimate of the PhSe–H BDE of  $75 \pm 3 \text{ kcal/mol}$  and an estimate of the PhTe–H BDE of  $70 \pm 3 \text{ kcal/mol}$ . The experimental data reported above led to an estimate of the PhSe–H bond strength of  $72 \pm 3 \text{ kcal/mol}$ , which overlaps with the theoretically derived value within experimental error. The kinetic observations described above led to the conclusion that the PhTe–H bond strength was  $\leq 63 \text{ kcal/mol}$ . That conclusion appears valid in view of the well-established H–Te bond strength in  $\text{H}_2\text{Te}$  of  $66 \text{ kcal/mol}$ , as shown in eq 1, and the expected weakening of the H–Te–Ph bond relative to H–Te–H (as discussed below). Therefore, it seems likely that the BDE calculated by our DFT methods is too high. Wright and co-workers (see ref 36) have shown that accurate H–X bond energies can be determined by these techniques for  $\text{X} = \text{C}, \text{N}, \text{O},$  and  $\text{S}$ . Facile extension to heavier elements remains a challenge to both theory and experiment.

Calculation of homolytic cleavage of the dichalcogenide bond, as shown in eq 26, was also studied computationally.



The calculated enthalpies of reaction 26 are surprising low:  $-1.3 \text{ kcal/mol}$  for Se and  $0.0 \text{ kcal/mol}$  for Te. As shown in Table 1, the experimental data reported in this paper yield estimates of  $46$ ,  $41$ , and  $33 \text{ kcal/mol}$  for the PhE–EPh bond in going from S to Se to Te. The computational value is again in reasonable accord with experimental data for Se; however, the calculational result that the PhTe–TePh bond has essentially the same strength as the PhS–SPh bond disagrees with the experimentally derived results.

A complicating factor in these calculations is the extent to which the chalcogenide radicals are stabilized by delocalization into antibonding orbitals of the aryl group. As mentioned in the Introduction, Benson has proposed a value of about  $17 \text{ kcal/mol}$  for O and about  $10 \text{ kcal/mol}$  for S. These factors tend to make the H–E–Ph bond weaker than the H–E–H bond as a result of stabilization of the  $\bullet\text{EPh}$

(36) The electronic energy  $\Delta E^0$  (0 K) referred to herein can potentially be corrected to yield  $\Delta H^0$  (298 K) according to methods discussed in the following reference: DiLabio, G. A.; Pratt, D. A.; LoFaro, A. D.; Wright, J. S. *J. Phys. Chem. A* **1999**, *103*, 1653. The required zero-point energy calculations were deemed too computationally intensive for our present purposes, and our presentation in terms of isodesmic reactions should lead to a maximum of error cancellation in any case.

(37) See note 29 of the following reference for the definition of  $S^2$  as implemented in ADF: Bulo, R. E.; Ehlers, A. W.; Grimme, S.; Lammertsma, K. *J. Am. Chem. Soc.* **2002**, *124*, 13903.

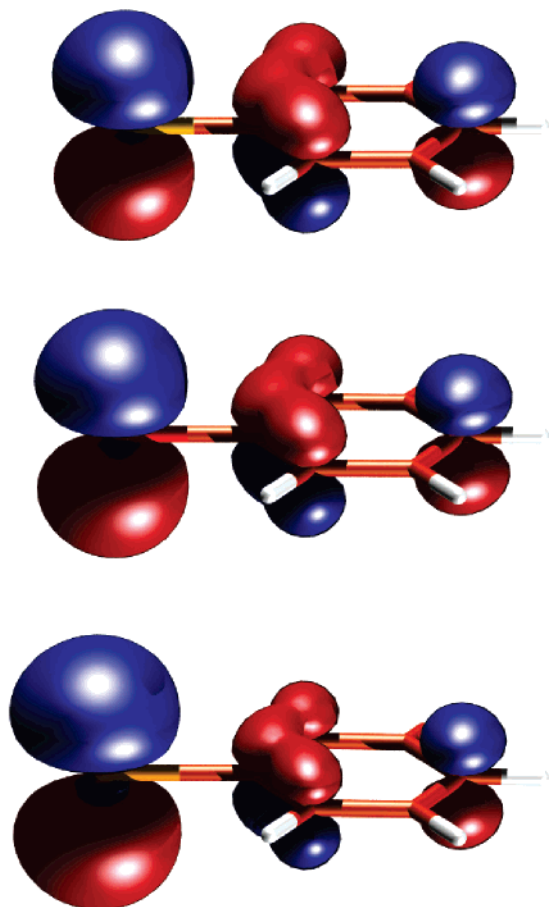


**Figure 6.** The calculated SOMO orbitals for SPh, SePh, and TePh from top to bottom, respectively. Note the increase in %E character on descending the column.

radical by donation from chalcogen to the  $\pi$  orbitals of the pendant arene. Results of our calculations show that the percentage of the SOMO that resides on the E atom decreases from 69.4 (Te) to 58.7(Se) to 51.4(S). Thus, the  $\bullet$ SPh radical shows the largest delocalization into the arene ring, and this presumably results in greater stabilization for it relative to the analogous Se and Te radicals. An additional observation from the computational study is that the SOMO is also the HOMO-1 (HOMO = highest occupied molecular orbital) for each of the three radicals; this non-Aufbau electron configuration is a consequence of the partial C–C  $\pi$ -bonding nature of the SOMO (see Figure 6). The HOMO, in contrast, is an in-plane lone pair of electrons residing in a nearly pure p orbital of the E atom, perpendicular to the C–E bond.

The chemical consequences of the changing nature of the SOMO calculated for these radicals are not clear at this time.

Additional work aimed at better defining the theoretical underpinnings to the chemistry of the heavier chalcogenides is called for.

### Conclusion

The main goal of this work was to generate PhE–EPh bond strengths, which can be of use in further studies of the reactivity of the chalcogenides. The PhE–EPh bond, as shown in Table 1, was found to decrease in strength: S = 46, Te = 41, Se = 33 kcal/mol. Experimental errors in these absolute bond strengths are high, on the order of  $\pm 3$  kcal/mol, but represent our best central data for these important bonds. In addition, estimates of the H–EPh bond were also found to decrease in this series: S = 81,<sup>6b</sup> Se = 72, Te = 63 kcal/mol. These data roughly parallel the accurate literature data for H–EH, as shown in eq 1. The low strength of the H–TePh bond has important kinetic consequences in that it is even weaker than the H–Cr bond strength, thus, interrupting the normal direction of H atom transfer from transition-metal hydride to main-group radical. The Cr–EPh bond strength also follows this order (S = 38, Se = 36, Te = 31), but the decrease is less marked; in particular, the gap in the Cr–SPh and Cr–SePh bond strengths is within experimental error. Initially, it was felt that this might be due to steric factors destabilizing the Cr–SPh bond; however, as shown in Figure 1, there is little sign of perturbation of the metal–ligand bonding framework in this molecule. As discussed earlier, the “soft” metal system, most notably the Cr–CO bonds, may act as a buffer and tend to stabilize the heavier chalcogenide bonds because they are less electro-negative and less electron withdrawing, resulting in somewhat stronger Cr–CO bonds, as indicated in the FTIR spectra in Figure 5. This is not believed to be a dominant effect; rather it is believed to be an attenuating effect. Additional kinetic, thermodynamic, and computational studies with other “harder” complexes will shed additional light on this question and are in progress.

**Acknowledgment.** For support of this work, the authors are grateful to the National Science Foundation (C.R.C.; Grant -0209977).

**Supporting Information Available:** Tables with bond lengths, bond angles, atomic coordinates, anisotropic displacement factors for Ph–S–Cr(CO)<sub>3</sub>( $\eta^5$ -C<sub>5</sub>Me<sub>5</sub>) and Ph–Se–Cr(CO)<sub>3</sub>( $\eta^5$ -C<sub>5</sub>Me<sub>5</sub>), tables of calculated geometries for PhEPh and PhEH, UV–vis and stopped-flow kinetic data, and graphs of fits to kinetic data for the reaction of PhSeH and Ph– $\bullet$ Cr(CO)<sub>3</sub>( $\eta^5$ -C<sub>5</sub>Me<sub>5</sub>). This information is available free of charge via the Internet at <http://pubs.acs.org>.

IC048321P